Photocatalytic norfloxacin degradation enabled by dual S-scheme nanocellulose-based Ag_2WO_4/NiO/MoO_3 tertiary heterojunction

Shabnam Sambyal[a], Vinay Chauhan[a], Pooja Shandilya[b,d]*, Aashish Priye[b,c]*

[a]*School of Advanced Chemical Sciences, Shoolini University, Solan, HP 173229, India*

[b]*Department of Chemical and Environmental Engineering, University of Cincinnati, Cincinnati, OH 45221, USA*

[c]*Digital Futures, University of Cincinnati, Cincinnati, OH 45221, USA*

[d]*Department of Chemistry, MMEC, Maharishi Markandeshwar (Deemed to be University), Mullana-Ambala, Haryana 133207, India*

**Corresponding Authors*: Aashish Priye and Pooja Shandilya

E-mail: *priyeah@ucmail.uc.edu* *and* *shandipj@ucmail.uc.edu*

Table S1: Previous reports on nanocellulose, Ag_2WO_4, NiO and MoO_3 based heterojunction for photodegradation application.

Photocatalyst	Pollutants	Photodegradation efficiency (In %)	Irradiation time (In min)	Migration	Recyclability	References
$ZnTiO_3$-nanocellulose	Tetrahydrochloride	98.27	120	-	5	[1]
Cellulose/γ-Fe_2O_3-ZrO_2	Congo Red	98.5	35	Type-II	4	[2]
MrGO/Ag_2WO_4	Lomefloxacin degradation	93.62	120	Z-scheme	4	[3]
Ag_2WO_4/ZIF-8	MB degradation	98.3	120	Z-scheme	5	[4]
Ag_2WO_4/BiOBr	Lanasol Red	98	15	Z-scheme	4	[5]
g-C_3N_4/Ag_2WO_4/Bi_2S_3	Congo Red	98	60	S-scheme	5	[6]
g-C_3N_4/BiOI/Ag_2WO_4	Sudan Red III	89	90	Z-scheme	5	[7]
NiO@Bi_2MoO_6-MoS_2	Indigo carmine	98.8	120	-	5	[8]
NiO/BiOI	Rhodamine B	-	-	S-scheme	5	[9]
NiO/BiOBr	Oxytetracycline and 2-Mercaptobenzothiazole	72.6 and 97.7	120 and 9	Z-scheme	4	[10]
Bi_2WO_6/NiO	Ciprofloxacin	92.5	90	S-scheme	-	[11]

3D-Bi_2MoO_6@MoO_3/PU	Oxytetracycline	88.89	20	Z-scheme	9	[12]
$ZnIn_2S_4$@MoO_3	Tetracycline hydrochloride	99.2	90	Z-scheme	4	[13]
ZnO/CuO/MoO_3	Rhodamine B and alizarin yellow	97 and 79	120	Type-II	5	[14]

Table S2: Comparative analysis of contemporary literature in recent years regarding the photocatalytic efficiency of NFX.

Photocatalyst	**Photocatalyst Dosages (In mg/L)**	**Pollutant concentration (In mg/L)**	**pH**	**Light source**	**Reactive species**	**Degradation efficacy (In %)**	**Time (In min)**	**Cycles**	**References**
NiO	10	50	10	Xe lamp	$\dot{O}H$ and h^+	-	40	-	[15]
MoO_3	50	20	-	300 W Xe lamp	$\dot{O}H$ and h^+	100	40	5	[16]
TiO_2	1000	-	1	Hg lamp	-	-	80	-	[17]
Mn:ZnS Quantum Dots	60	15	10	Hg lamp	e^-, $\dot{O}_2^-$ and $\dot{O}H$	86	60	4	[18]
Ce-TiO_2 and B-TiO_2	500 and 1000	10	7	Under sunlight	h^+ and e^-	93	180	5	[19]
Ag_3PO_4/graphene oxide	-	15	-	250 W Xe lamp	h^+ and $\dot{O}_2^-$	83.68	100	4	[20]

$Bi_2Sn_2O_7/g\text{-}C_3N_4$	20	20	-	500 W Xe lamp	e^- and h^+	94	3 h	5	[21]
LaOCl/LDH	20	10	7	300 W Xe lamp	$^{\cdot}O_2^-$	90	150	3	[22]
$ZnFe_2O_4/BiOBr$	-	50	-	300 W Xe lamp	h^+ and $^{\cdot}O_2^-$	91.70	60	5	[23]
$NiWO_4@g\text{-}C_3N_4$	50	10	-	W lamp	$^{\cdot}OH$ and h^+	97	60	5	[24]
In_2O_3/TiO_2	30	20	-	500 W Xe lamp	$^{\cdot}OH$	100	10	45	[25]
ZnO/ZnS	25	25	7	UV lamp	$^{\cdot}O_2^-$	95	3 h	5	[26]
NiO/ZnO	30	10 μM	-	W lamp	$^{\cdot}O_2^-$ and h^+	96.73	80	5	[27]
$GDQ\text{-}MoS_2@Co_3O_4$	20	20	9	150 W Xe lamp	e^- and $^{\cdot}O_2^-$	99.3	90	4	[28]
NC-ANM	**15**	**50**	**6**	**LED bulb 50W**	**$^{\cdot}OH$ and $^{\cdot}O_2^-$**	**99.6**	**30**	**7**	**Present work**

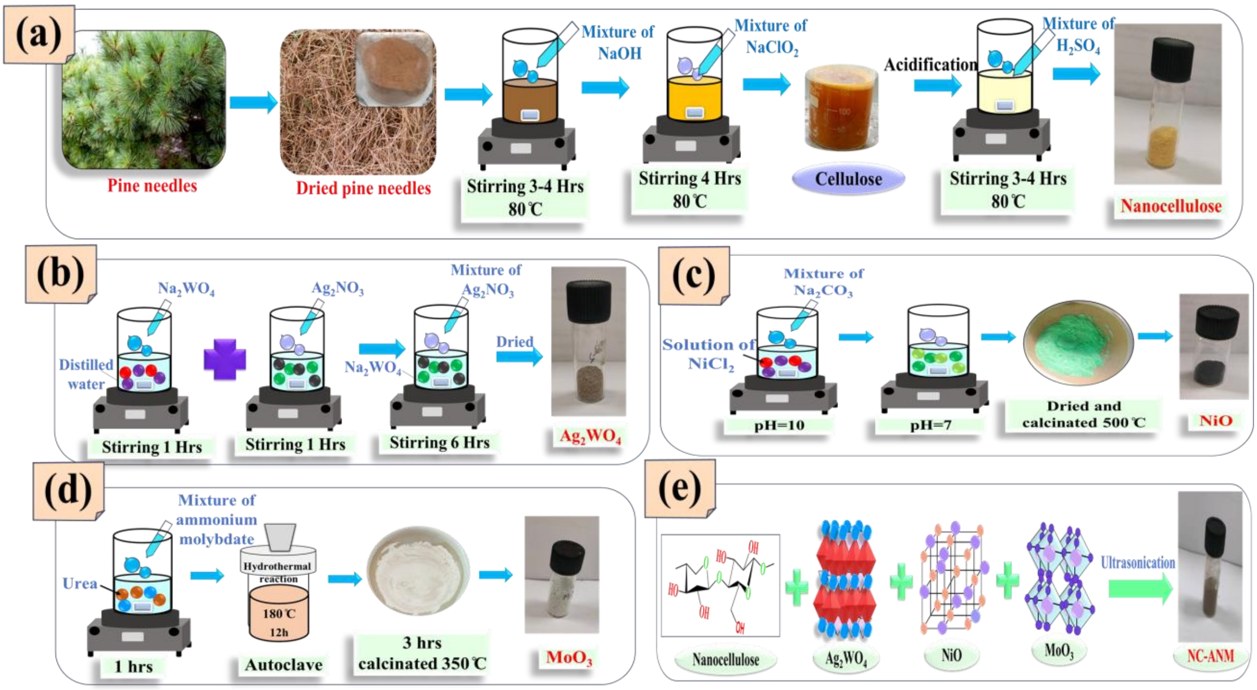

Scheme 1. Schematic diagram for the formation of (a) nanocellulose, (b) Ag_2WO_4, (c) NiO, (d) MoO_3, and (e) NC-ANM heterojunction.

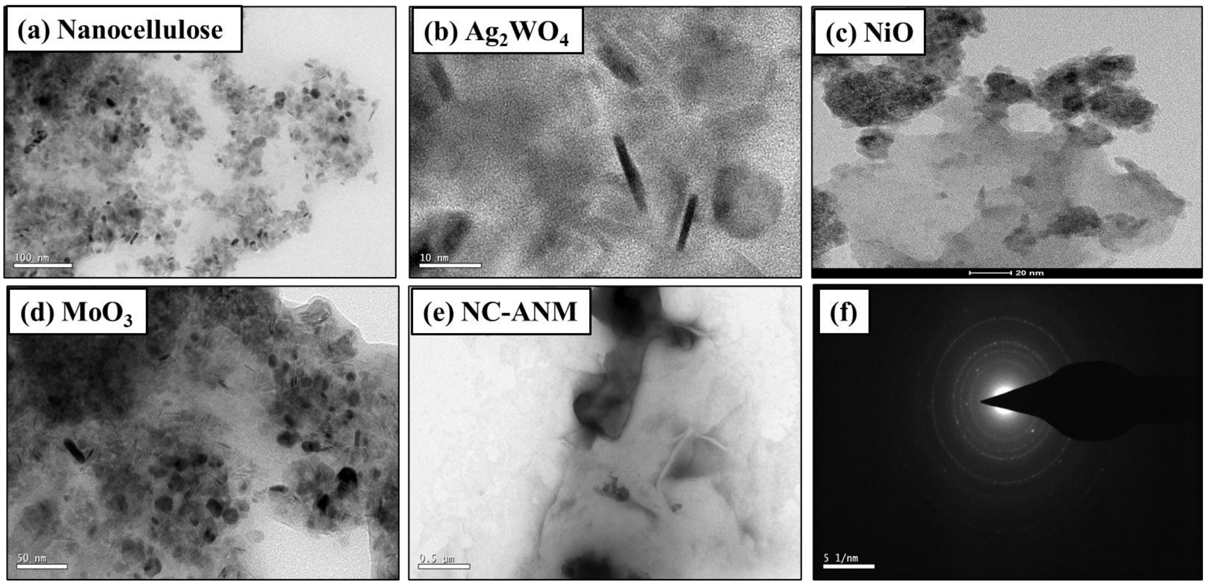

Figure S1. HRTEM result of (a) nanocellulose, (b) Ag_2WO_4, (c) NiO,(d) MoO_3, (e) NC-ANM heterojunction, and (f) SAED pattern of NC-ANM. Nanocellulose, Ag_2WO_4, NiO, and MoO_3 are granular, irregular-size rods, block sheets, and rod-like morphology with size 10-50 nm and NC-ANM, indicating its polycrystalline nature.

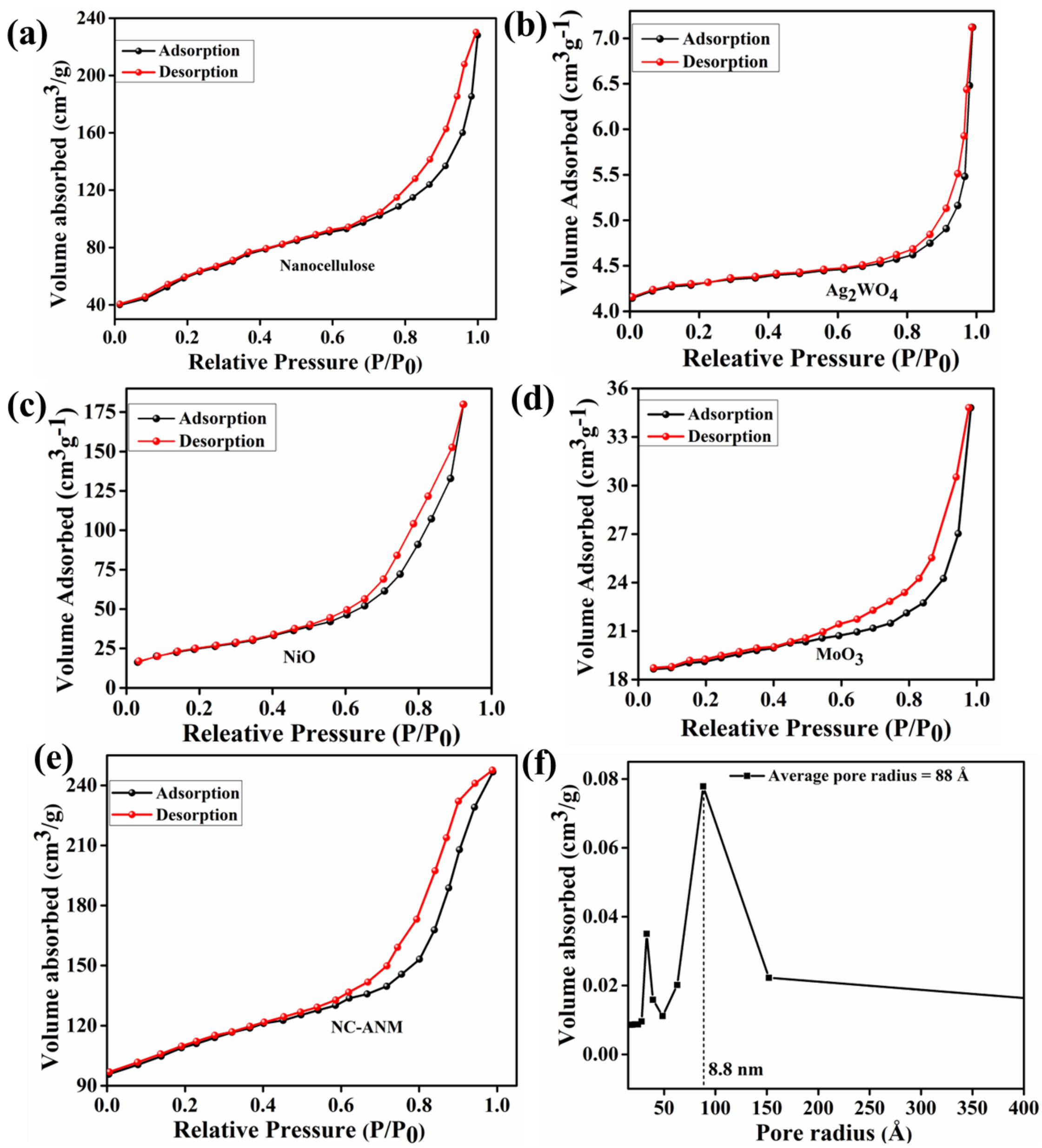

Figure S2. BET analysis of (a) nanocellulose, (b) Ag_2WO_4, (c) NiO, (d) MoO_3, (e) NC-ANM heterojunction, and (f) pore size distribution of NC-ANM. N_2 adsorption-desorption isotherm and pore size distribution of the NC-ANM composite, revealing its mesoporous structure with a high surface area and a narrow pore size distribution, beneficial for photocatalytic applications.

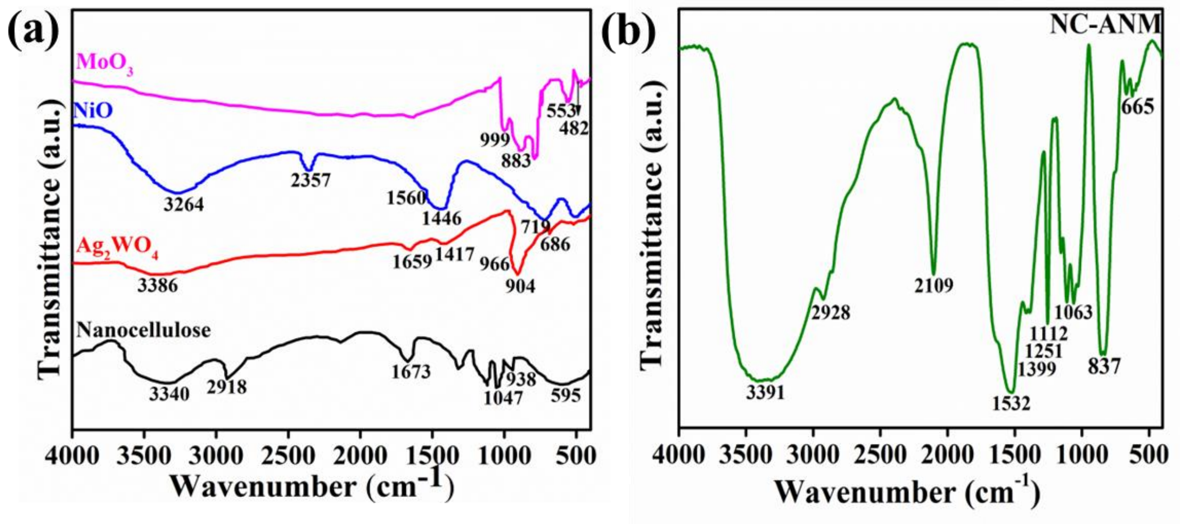

Figure S3. FTIR spectra of (a) nanocellulose, Ag_2WO_4, NiO, MoO_3, and (b) NC-ANM heterojunction.

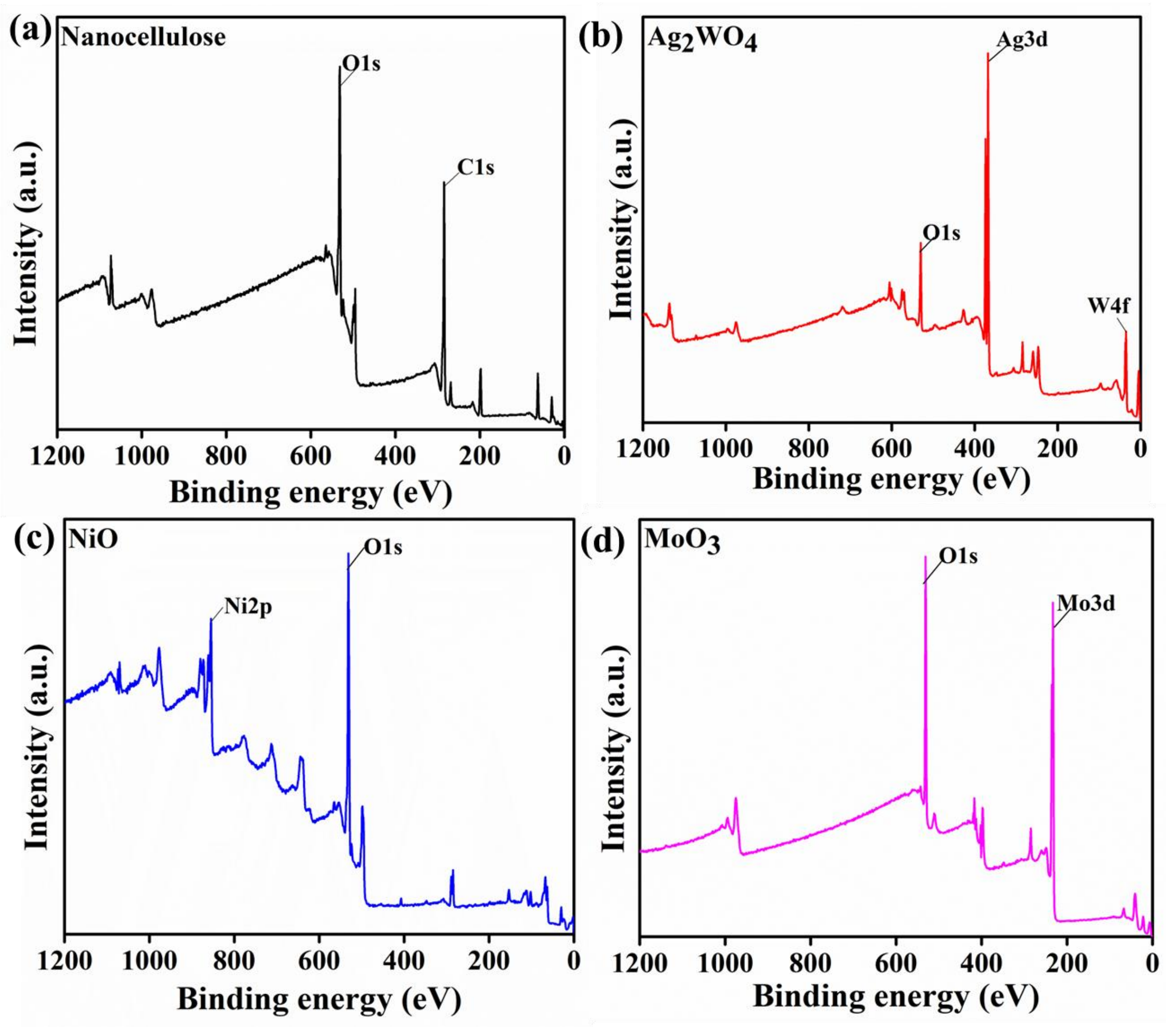

Figure S4. XPS survey of (a) nanocellulose, (b) Ag_2WO_4, (c) NiO, and (d) MoO_3.

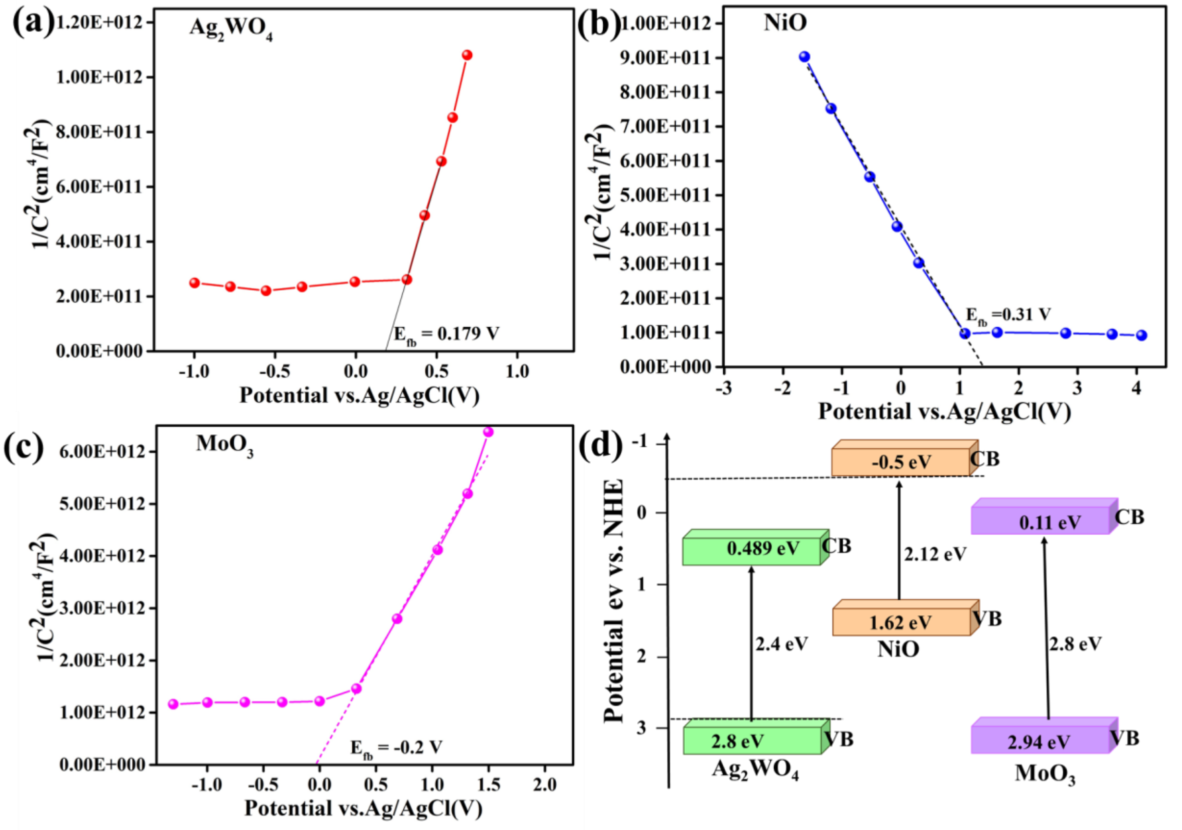

Figure S5. Mott-Schottky plots for bare (a) n-type Ag_2WO_4, (b) p-type NiO, (c) n-type MoO_3, and (d) Band structure of ANM heterojunction.

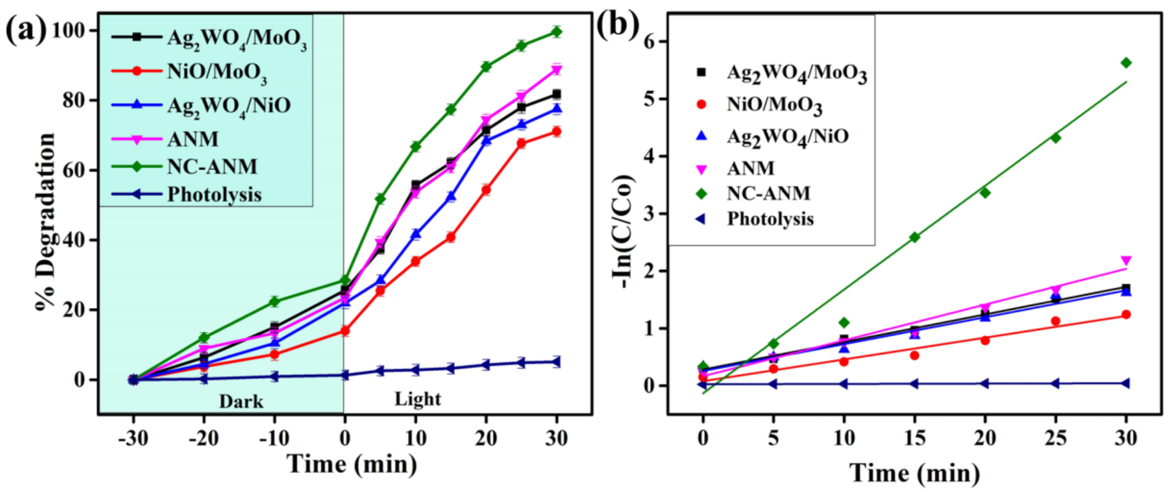

Figures S6. (a) Degradation percentage for binary heterojunction in possible combination and NC-ANM heterojunction, and (b) The kinetic analysis indicates that the reaction follows a pseudo-first-order model where NC-ANM heterojunction exhibits the highest rate constant.

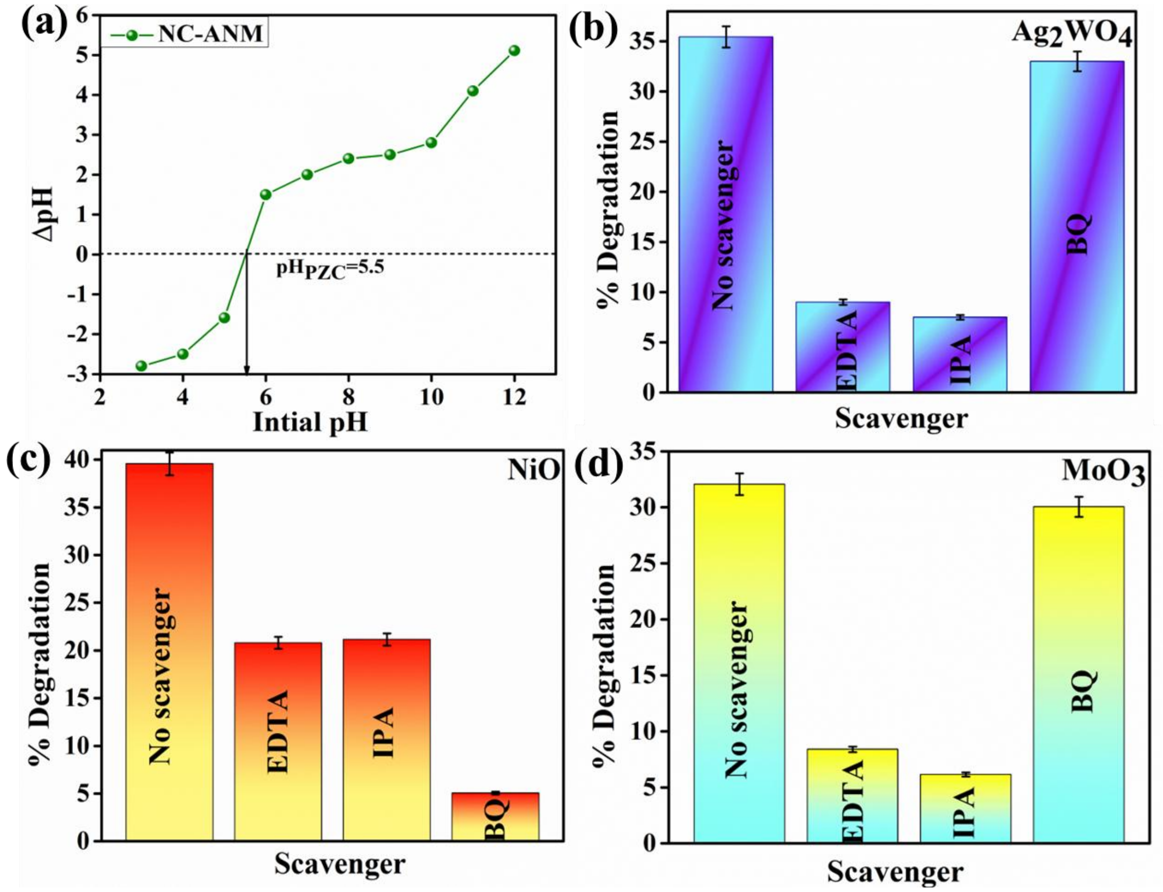

Figure S7. (a) Zero-point charge of NC-ANM heterojunction, (b) Trapping experiment for photodegradation of NFX using bare Ag_2WO_4, (c) NiO, and (d) MoO_3.

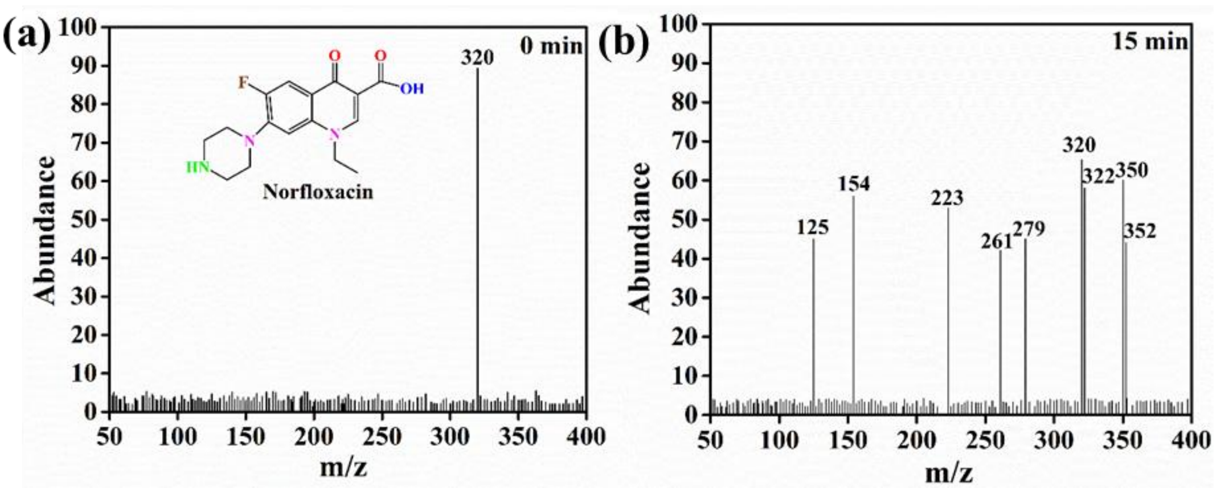

Figure S8. Liquid chromatography-mass spectrometry (LC-MS) chromatograms of NFX degradation at (a) time = 0 mins, and (b) time = 15 mins.

References

1. Gogoi, J. and D. Chowdhury, *Photodegradation of emerging contaminant tetracycline using a zinc titanate nanocellulose composite as an efficient photocatalyst.* Materials Advances, 2023. **4**(9): p. 2088-2098.
2. Helmiyati, H., et al., *Green hybrid photocatalyst containing cellulose and γ–Fe2O3–ZrO2 heterojunction for improved visible-light driven degradation of Congo red.* Optical Materials, 2022. **124**: p. 111982.
3. Sun, Y., et al., *Efficient removal of lomefloxacin by Z-scheme MrGO/Ag2WO4 heterojunction recyclable composite under visible light: Mechanism of adsorption and photodegradation.* Journal of Environmental Chemical Engineering, 2022. **10**(1): p. 107120.
4. Mohammed, R.O., et al., *Enhanced photocatalytic degradation activity of ZIF-8 doped with Ag2WO4 photocatalyst.* Journal of the Taiwan Institute of Chemical Engineers, 2023. **151**: p. 105141.
5. Fu, S., et al., *Facile fabrication of Z-scheme Ag2WO4/BiOBr heterostructure with oxygen vacancies for improved visible-light photocatalytic performance.* Journal of Science: Advanced Materials and Devices, 2023. **8**(2): p. 100561.
6. Jabbar, Z.H., et al., *Photocatalytic destruction of Congo red dye in wastewater using a novel Ag2WO4/Bi2S3 nanocomposite decorated g-C3N4 nanosheet as ternary S-scheme heterojunction: Improving the charge transfer efficiency.* Diamond and Related Materials, 2023. **133**: p. 109711.
7. Liao, Y., et al., *A novel g-C3N4/BiOI/Ag2WO4 heterojunction for efficient degradation of organic pollutants under visible light irradiation.* Ceramics International, 2021. **47**(18): p. 26248-26259.
8. Nandisha, P. and S. Yallappa, *Synthesis and characterization of ternary NiO@ Bi2MoO6–MoS heterojunction with enhanced photodegradation efficiency towards indigo carmine dye.* Solid State Sciences, 2023. **139**: p. 107157.
9. Hu, X., et al., *Step-scheme NiO/BiOI heterojunction photocatalyst for rhodamine photodegradation.* Applied Surface Science, 2020. **511**: p. 145499.
10. Dong, J., et al., *Construction of Z-scheme NiO/BiOBr heterojunction for facilitating photocatalytic degradation of oxytetracycline and 2-mercaptobenzothiazole.* Journal of Alloys and Compounds, 2024. **976**: p. 172920.

11. Li, Z., et al., *Bi-functional S-scheme S-Bi2WO6/NiO heterojunction for photocatalytic ciprofloxacin degradation and CO2 reduction: Mechanisms and pathways.* Separation and Purification Technology, 2023. **310**: p. 123197.
12. Liu, Y., et al., *Stable photodegradation of antibiotics by the functionalized 3D-Bi2MoO6@ MoO3/PU composite sponge: High efficiency pathways, optical properties and Z-scheme heterojunction mechanism.* Chemosphere, 2023. **332**: p. 138911.
13. Ouyang, C., et al., *Direct Z-scheme ZnIn2S4@ MoO3 heterojunction for efficient photodegradation of tetracycline hydrochloride under visible light irradiation.* Chemical Engineering Journal, 2021. **424**: p. 130510.
14. Hussain, M.K., et al., *Enhanced visible light-driven photocatalytic activity and stability of novel ternary ZnO/CuO/MoO3 nanorods for the degradation of rhodamine B and alizarin yellow.* Materials Science in Semiconductor Processing, 2023. **155**: p. 107261.
15. PARIMALA, L. and J. SANTHANALAKSHMI, *Synthesis, Characterisation and Catalytic Behaviour of NiO Nanoflowers for the Photo Degradation of Norflaxacin in Aqueous Medium.* Chemical Science, 2019. **8**(1): p. 70-76.
16. Huang, Y., et al., *Molybdenum oxide nanorods decorated with molybdenum phosphide quantum dots for efficient photocatalytic degradation of rhodamine B and norfloxacin.* Research on Chemical Intermediates, 2022. **48**(7): p. 2887-2901.
17. Haque, M. and M. Muneer, *Photodegradation of norfloxacin in aqueous suspensions of titanium dioxide.* Journal of Hazardous materials, 2007. **145**(1-2): p. 51-57.
18. Patel, J., A.K. Singh, and S.A. Carabineiro, *Assessing the photocatalytic degradation of fluoroquinolone norfloxacin by Mn: ZnS quantum dots: Kinetic study, degradation pathway and influencing factors.* Nanomaterials, 2020. **10**(5): p. 964.
19. Manasa, M., P.R. Chandewar, and H. Mahalingam, *Photocatalytic degradation of ciprofloxacin & norfloxacin and disinfection studies under solar light using boron & cerium doped TiO2 catalysts synthesized by green EDTA-citrate method.* Catalysis today, 2021. **375**: p. 522-536.
20. Ji, B., et al., *Immobilized Ag 3 PO 4/GO on 3D nickel foam and its photocatalytic degradation of norfloxacin antibiotic under visible light.* RSC advances, 2020. **10**(8): p. 4427-4435.

21. Zhu, Z., et al., *Facile Construction of Bi2Sn2O7/g-C3N4 Heterojunction with Enhanced Photocatalytic Degradation of Norfloxacin.* Inorganics, 2022. **10**(9): p. 131.
22. Zhang, W., et al., *Boosted photocatalytic degradation of norfloxacin on LaOCl/LDH: Synergistic effect of Z-scheme heterojunction and O vacancies.* Journal of Environmental Chemical Engineering, 2022. **10**(3): p. 107812.
23. Meng, X., et al., *Preparation and visible light catalytic degradation of magnetically recyclable ZnFe2O4/BiOBr flower-like microspheres.* Journal of Alloys and Compounds, 2023. **954**: p. 169981.
24. Muthuraj, V., *Superior visible light driven photocatalytic degradation of fluoroquinolone drug norfloxacin over novel NiWO4 nanorods anchored on g-C3N4 nanosheets.* Colloids and Surfaces A: Physicochemical and Engineering Aspects, 2019. **567**: p. 43-54.
25. Yu, H., et al., *Enhanced photocatalytic degradation of norfloxacin under visible light by immobilized and modified In2O3/TiO2 photocatalyst facilely synthesized by a novel polymeric precursor method.* Journal of Materials Science, 2019. **54**(14): p. 10191-10203.
26. Liu, W., et al., *Synergistic adsorption-photocatalytic degradation effect and norfloxacin mechanism of ZnO/ZnS@ BC under UV-light irradiation.* Scientific Reports, 2020. **10**(1): p. 11903.
27. Arunpandian, M., et al., *Visible-Light Induced Degradation of Norfloxacin and Methylene Blue Using Easily Recoverable NiO/ZnO Heterostructures: Analysis of Efficacy, Stability, Reaction Mechanism and Degradation Pathway.* Journal of Inorganic and Organometallic Polymers and Materials, 2023: p. 1-14.
28. Adhikari, S., S. Mandal, and D.-H. Kim, *pn Junction catalysis in action: Boosting norfloxacin photodegradation with ZIF-67-based Co3O4 wrapped in MoS2 with surface functionalized graphene quantum-dot.* Applied Surface Science, 2024. **653**: p. 159374.